

Self-assembled CdS/Au/ZnO heterostructure induced by surface polar charges for efficient photocatalytic hydrogen evolution†

Cite this: *J. Mater. Chem. A*, 2013, **1**, 2773

Received 13th December 2012
Accepted 14th January 2013

DOI: 10.1039/c3ta01476b

www.rsc.org/MaterialsA

Zong Bao Yu,^{‡a} Ying Peng Xie,^{‡a} Gang Liu,^{*a} Gao Qing (Max) Lu,^b Xiu Liang Ma^a and Hui-Ming Cheng^a

A ternary heterostructure of CdS/Au/ZnO, where a core-shell structure of Au/CdS is selectively deposited on the polar surface of ZnO induced by the surface polar charges of ZnO crystals, is prepared through a two-step self-assembly process. The resultant heterostructure shows an activity 4.5 times higher in photocatalytic hydrogen evolution from water containing Na₂S/Na₂SO₃ electron donors than the binary CdS/ZnO heterostructure as a result of the effective vectorial Z-scheme transfer of photogenerated charge carriers between ZnO and CdS mediated by Au nanoparticles at the interface.

Photocatalytic hydrogen evolution from water using semiconductors represents a very attractive pathway for converting solar energy to chemical energy. In order to acquire high energy conversion efficiency, worldwide efforts have been devoted to developing various efficient photocatalysts.^{1,2} ZnO with a direct bandgap of 3.3 eV and an exciton binding energy of 60 meV has been actively investigated as a photocatalyst due to the merits of its high electron mobility, abundant morphologies, easy synthesis, low cost and non-toxicity.^{3,4} The application of ZnO as a photocatalyst is, however, hindered by some apparent drawbacks: (i) the fast recombination rate of photogenerated electron-hole pairs; (ii) the narrow light responsive range; and (iii) serious photocorrosion. To address these drawbacks, many strategies such as doping,^{5,6} loading noble metals,^{7,8} and coupling with other semiconductors^{9–12} have been used. Constructing heterostructures has attracted increasing attention

due to the versatility of extending the light absorption range, promoting the separation of photogenerated charge carriers in photocatalysts and also improving the stability.

ZnO based heterostructures including TiO₂/ZnO,⁹ CuO/ZnO¹⁰ and CdSe/ZnO¹¹ have been actively studied and exhibit the ability to improve the photocatalytic activity of ZnO photocatalysts. These heterostructures serve the function of transferring the photoexcited electrons from the semiconductor with a high conduction band (CB) to the other with a low CB (the traditional charge-carrier transfer process). On the other hand, ZnO/CdS heterostructures with an improved photocatalytic H₂ evolution follow a different charge-carrier transfer mechanism, namely the direct Z-scheme, where the recombination of the photoexcited electrons from the ZnO CB and holes from the CdS valence band (VB) occurs at the interface.¹² In this case, the photoexcited electrons in CdS with a high CB and holes in ZnO with a low VB can be retained. The direct Z-scheme is favorable for generating photoexcited charge carriers with high energy, which is desirable for photocatalysis in terms of thermodynamic requirements.

In principle, the direct Z-scheme related charge-carrier transfer process should compete with the traditional charge-carrier transfer process in a CdS/ZnO heterostructure. It is therefore important to promote the direct Z-scheme charge-carrier transfer process by creating a favorable interface. Early studies showed that the interface containing a metallic polar surface of ZnO is favorable for improving the performance of the heterostructures as a result of a strengthened direct Z-scheme transfer process.¹³ Tada *et al.* have reported that Au nanoparticles can act as an electron transfer mediator to promote vectorial electron transfer between TiO₂ and CdS,¹⁴ which can have the same effect as the direct Z-scheme. Similar results were also demonstrated in the nanosized heterostructure of CdS/ZnO constructed on the microsized metallic core of Cd.¹⁵ All this progress suggests that the metallic or metal containing interface of the CdS/ZnO heterostructure is highly important for promoting the direct Z-scheme charge-carrier transfer process and thus photocatalytic H₂ evolution from water.

^aShenyang National Laboratory for Materials Science, Institute of Metal Research, Chinese Academy of Sciences, 72 Wenhua RD, Shenyang 110016, China. E-mail: gangliu@imr.ac.cn

^bARC Centre of Excellence for Functional Nanomaterials, The University of Queensland, Qld. 4072, Australia

† Electronic supplementary information (ESI) available: (1) Experimental section. (2) XRD patterns of ZnO, CdS/ZnO and CdS. (3) SEM images of Au/ZnO and CdS/ZnO. (4) XPS spectra of CdS/Au/ZnO. (5) SEM image and XRD patterns of CdS/Au/ZnO after reactions. See DOI: 10.1039/c3ta01476b

‡ These authors contributed equally to this work.

The structure of wurtzite-type ZnO crystals can be simply described as a number of alternating planes of O^{2-} and Zn^{2+} ions stacked along the c -axis. This means that some surfaces of ZnO crystals are terminated entirely with O^{2-} anions or Zn^{2+} cations, resulting in negatively or positively charged surfaces, namely polar surfaces.³ The typical polar surfaces in ZnO crystals are the O-terminated $(000\bar{1})$ and Zn-terminated (0001) . They have unusual properties in selectively adsorbing reaction molecules or ions as a result of electrostatic interactions, which makes it possible to construct some targeted heterostructures on the polar surfaces. For example, Joo *et al.* showed that positively charged Cd based complex ions are preferentially adsorbed on the negatively charged polar face $(000\bar{2})$.¹⁶ It is therefore expected that metal-CdS architectures might be formed on the metallic polar surface. The interface consisting of both a metallic polar surface of ZnO and a metal core should facilitate the occurrence of the direct Z-scheme in a CdS/ZnO heterostructure.

Here, we report the construction of a ternary CdS/Au/ZnO heterostructure for improving photocatalytic H_2 evolution from water, where both Au and CdS nanoparticles are selectively deposited on the polar surfaces of ZnO crystals. The schematic of the preparation route of the heterostructure is given in Fig. 1. The basis of constructing such an unusual heterostructure is the electrostatic adsorption of Cd and Au based complex ions on the polar surfaces of ZnO nanosheets. In detail, Au based complex ions are first preferentially adsorbed on the negatively charged O- $(000\bar{1})$ of ZnO, and subsequently a photodeposition process leads to the formation of Au nanoparticles on the polar surface. The CdS nanoparticles are then deposited on the Au pre-deposited O- $(000\bar{1})$ surface by a combination of preferential adsorption of Cd^{2+} ions and chemical bath deposition.

The ZnO crystals used in this work were synthesized by a modified hydrothermal process with sodium hydroxide (NaOH) and trisodium citrate dehydrate (TCD) as the morphology controlling agents according to an early report by Zeng *et al.*¹⁷ The X-ray diffraction pattern confirms the resultant crystals to be a pure ZnO phase with a wurtzite structure (Fig. S1a†). The scanning electron microscopy (SEM) image in Fig. 2a shows that ZnO crystals have the morphology of flower-like spheres with an average diameter of *ca.* 5 μm . These spheres are built by relatively uniform nanosheets with a thickness of *ca.* 100 nm (Fig. 2b). The transmission electron microscopy (TEM) image and selected area electron diffraction (SAED) pattern of a single

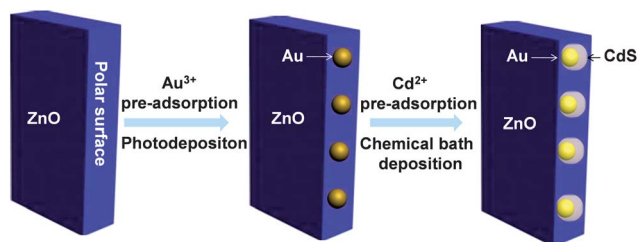


Fig. 1 Schematic of the preparation route of a CdS/Au/ZnO heterostructure through a two-step self-assembly process induced by the surface polar charges of ZnO.

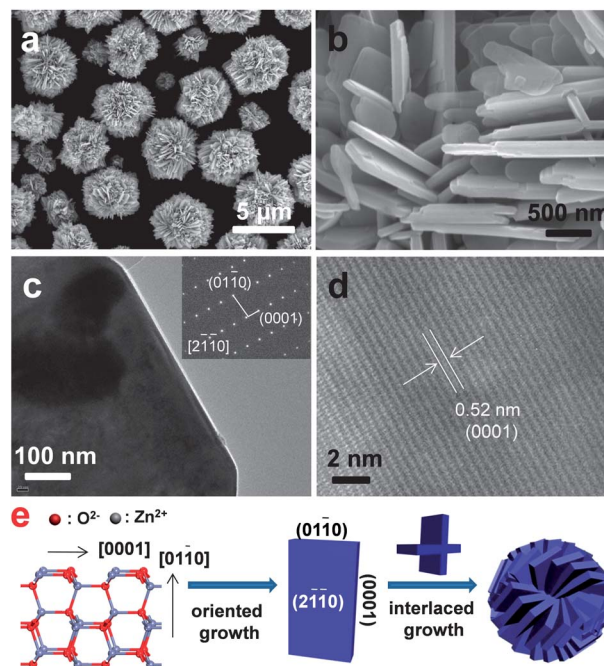


Fig. 2 (a and b) Low-magnification and high-magnification SEM images of flower-like spheres of ZnO crystals; (c and d) TEM and high-resolution TEM images of a single ZnO nanosheet. The inset in (c) is a corresponding SAED pattern; (e) schematic of the formation process of a flower-like ZnO sphere.

nanosheet are given in Fig. 2c. The SAED pattern suggests the single crystalline nature of the nanosheet. The lattice fringes with a distance of 0.52 nm in a high-resolution TEM image recorded along the $[2\bar{1}10]$ zone (Fig. 2d) is assigned to the $(000\bar{1})$ or (0001) planes, indicating that a ZnO nanosheet surface consists of a major top plane $(2\bar{1}\bar{1}0)$ and minor lateral polar planes of $(000\bar{1})/(0001)$ and $(01\bar{1}0)$. The anisotropic shape of the nanosheets can be understood as the preferential growth of the crystals along the $[0001]$ and $[01\bar{1}0]$ directions with the assistance of a morphology controlling agent, as demonstrated in Fig. 2e.¹⁸ The agglomeration growth of these nanosheet units into the final flower-like spheres is probably driven by the electrostatic attraction among the polar surfaces. After that, the nanosheets would interlace with each other to form the final flower-like ZnO structure.

The selective deposition of Au and CdS nanoparticles on the polar surfaces of ZnO crystals was conducted as follows. The synthesized ZnO powder was suspended in an aqueous solution of $AuCl_3$ in the dark to ensure the pre-adsorption of Au based complex ions on the polar surfaces of ZnO. Under UV irradiation, nearly all the Au nanoparticles were selectively deposited on the lateral polar surfaces of ZnO (Fig. 3a). X-ray energy dispersive spectrometer images (the inset in Fig. 3a and Fig. S2†) confirm the deposition of Au on ZnO. The selective distribution of Au nanoparticles with a size of 10–20 nm can be doubly confirmed in the TEM image (Fig. 3b). The pre-adsorption of Cd^{2+} based complex ions on the ZnO crystals was conducted by suspending the sample in an aqueous solution of $Cd(CH_3CO_2)_2$. The addition of thiourea to the suspension and subsequent chemical bath deposition at 80 °C resulted in the deposition of

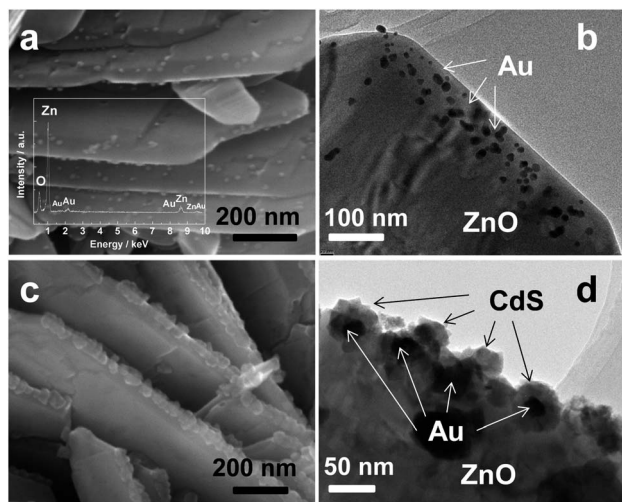


Fig. 3 (a and b) SEM and TEM images of Au/ZnO; (c and d) SEM and TEM images of the CdS/Au/ZnO heterostructures. The inset in (a) is the EDS spectrum of Au/ZnO.

CdS nanoparticles on the lateral polar surfaces of ZnO crystals (Fig. S3[†]). The crystal structure of CdS nanoparticles in the CdS/ZnO heterostructure is confirmed to be hexagonal (Fig. S1b and c[†]). Similar CdS nanoparticles with a size of *ca.* 50 nm can be further deposited on the Au deposited polar surfaces as shown in Fig. 3c, suggesting that the pre-deposition of Au nanoparticles on the polar surfaces has a negligible influence on the subsequent deposition of CdS. It is revealed by the TEM image in Fig. 3d that the subsequently deposited CdS nanoparticles cover most of the Au nanoparticles. XPS spectra further confirm the compositions of CdS/Au/ZnO (Fig. S4[†]). Therefore, the expected architecture of Au/CdS is rationally constructed on the polar surfaces of ZnO crystals.

The photocatalytic activity of the CdS/Au/ZnO heterostructure was investigated by monitoring hydrogen evolution from water with $\text{Na}_2\text{S}/\text{Na}_2\text{SO}_3$ as the sacrificial agent. Compared to the CdS/ZnO heterostructure, the heterostructure of CdS/Au/ZnO shows remarkably improved photocatalytic hydrogen evolution by a factor of 4.5 ($60.8 \mu\text{mol h}^{-1}$ vs. $13.4 \mu\text{mol h}^{-1}$). As demonstrated in Fig. 3d, a very small portion of Au nanoparticles are exposed without CdS coating. So it is useful to estimate the effect of the exposed Au nanoparticles on photocatalytic activity considering the possible cocatalyst function of noble metals.¹⁹ To clarify this issue, 1 wt% Au nanoparticles were loaded on the heterostructure of CdS/ZnO by the photo-deposition method (denoted as Au/CdS/ZnO). It is found that the hydrogen evolution rate of CdS/ZnO only increases from 13.4 to $19.7 \mu\text{mol h}^{-1}$ with the loading of Au nanoparticles, suggesting that some exposed Au nanoparticles in the CdS/Au/ZnO heterostructure do not contribute to the observed activity improvement (Fig. 4). Therefore, the introduced Au nanoparticles in the CdS/ZnO interface should be responsible for the improvement by strengthening the interface charge-carrier transfer between CdS and ZnO. In addition, both the morphology and the flower-like structure of ZnO particles can be retained after photocatalytic reactions (Fig. S5[†]).

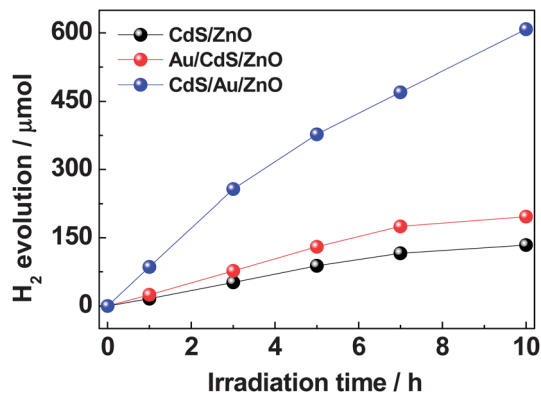


Fig. 4 Time courses of photocatalytic H_2 evolution from water with the CdS/ZnO, Au/CdS/ZnO and CdS/Au/ZnO photocatalysts. Reaction conditions: 100 mg of photocatalyst was suspended in 270 mL aqueous solution with 0.1 M Na_2SO_3 and 0.1 M Na_2S .

The strengthened interface charge-carrier transfer can be evidenced by photoluminescence (PL) emission spectroscopy. Fig. 5 compares the PL emission spectra of ZnO, CdS/ZnO and CdS/Au/ZnO. Pure ZnO exhibits a narrow UV emission with its peak at 390 nm and a broad orange emission with its peak at 640 nm. The UV emission band is due to near band-edge transition, and the orange emission originates from defect emission in ZnO crystals.^{4,20} Although the CdS/ZnO heterostructure gives similar PL emission bands to ZnO, the band intensity is much weakened. For the CdS/Au/ZnO heterostructure the PL emission bands almost disappear. It is established that the charge-carrier transfer between different parts of composites usually results in the weakening of PL emission bands.²¹ In our case, the direct Z-scheme interface charge-carrier transfer (Fig. 6a) should be responsible for the weakened PL emission bands of the CdS/ZnO. The effective vectorial Z-scheme charge-carrier transfer process mediated by the Au nanoparticles at the interface as illuminated in Fig. 6b can well explain the quenching of PL emission in CdS/Au/ZnO. As a consequence, the high energy electrons and holes, remaining on the CdS CB and ZnO VB,

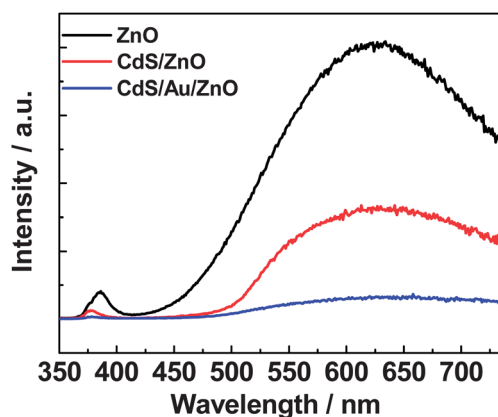


Fig. 5 Photoluminescence spectra of ZnO, CdS/ZnO and CdS/Au/ZnO recorded at room temperature with a 270 nm excitation wavelength.

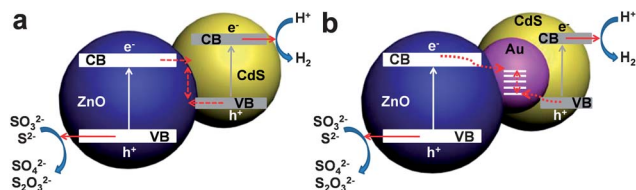


Fig. 6 Schematic of (a) the direct Z-scheme charge-carrier transfer process in the CdS/ZnO heterostructure and (b) the vectorial Z-scheme charge-carrier transfer process in the CdS/Au/ZnO heterostructure.

respectively, can be involved effectively in photocatalytic reactions for hydrogen evolution from water.

Conclusions

A core-shell structure of Au/CdS was selectively deposited on the polar surfaces of ZnO crystals through a two-step self-assembly process induced by surface polar charges. The heterostructure of CdS/Au/ZnO shows a much improved photocatalytic hydrogen evolution rate from water containing electron donors compared to CdS/ZnO or Au/CdS/ZnO heterostructures. The origin of this improvement lies in the formation of effective vectorial Z-scheme charge-carrier transfer at the interface of the CdS/Au/ZnO with Au as a mediator.

Acknowledgements

The authors thank the Major Basic Research Program, Ministry of Science and Technology of China (No. 2009CB220001), NSFC (No. 50921004, 51002160, 21090343 and 51172243), Solar Energy Initiative and the Funding (KJCX2-YW-H21-01) of the Chinese Academy of Sciences for financial support. GL thanks the IMR SYNL-T.S. Kê Research Fellowship.

References

1 A. Kudo and Y. Miseki, *Chem. Soc. Rev.*, 2009, **38**, 253.

- 2 H. M. Chen, C. K. Chen, R. S. Liu, L. Zhang, J. Zhang and D. P. Wilkinson, *Chem. Soc. Rev.*, 2012, **41**, 5654.
- 3 Z. L. Wang, *Mater. Sci. Eng., R*, 2009, **64**, 33.
- 4 A. B. Djurišić, X. Chen, Y. H. Leung and A. M. C. Ng, *J. Mater. Chem.*, 2012, **22**, 6526.
- 5 S. W. Liu, C. Li, J. G. Yu and Q. J. Xiang, *CrystEngComm*, 2011, **13**, 2533.
- 6 M. Mapa and C. S. Gopinath, *Chem. Mater.*, 2009, **21**, 351.
- 7 W. W. Lu, S. Y. Gao and J. J. Wang, *J. Phys. Chem. C*, 2008, **112**, 16792.
- 8 K. X. Yao, X. Liu, L. Zhao, H. C. Zeng and Y. Han, *Nanoscale*, 2011, **3**, 4195.
- 9 Y. C. Huang, S. Y. Chang, C. F. Lin and W. J. Tseng, *J. Mater. Chem.*, 2011, **21**, 14056.
- 10 S. Jung and K. Yong, *Chem. Commun.*, 2011, **47**, 2643.
- 11 S. Cho, J. W. Jang, J. Kim, J. S. Lee, W. Choi and K. H. Lee, *Langmuir*, 2011, **27**, 10243.
- 12 X. Wang, G. Liu, Z. G. Chen, F. Li, L. Wang, G. Q. Lu and H. M. Cheng, *Chem. Commun.*, 2009, 3452.
- 13 X. W. Wang, L. C. Yin, G. Liu, L. Z. Wang, R. Saito, G. Q. (Max) Lu and H. M. Cheng, *Energy Environ. Sci.*, 2011, **4**, 3976.
- 14 H. Tada, T. Mitsui, T. Kiyonaga, T. Akita and K. Tanaka, *Nat. Mater.*, 2006, **5**, 782.
- 15 X. W. Wang, G. Liu, L. Z. Wang, Z. G. Chen, G. Q. (Max) Lu and H. M. Cheng, *Adv. Energy Mater.*, 2012, **2**, 42.
- 16 J. Joo, B. Y. Chow, M. Prakash, E. S. Boyden and J. M. Jacobson, *Nat. Mater.*, 2011, **10**, 596.
- 17 J. H. Zeng, B. B. Jin and Y. F. Wang, *Chem. Phys. Lett.*, 2009, **472**, 90.
- 18 B. X. Li and Y. F. Wang, *J. Phys. Chem. C*, 2010, **114**, 890.
- 19 J. W. Chiou, S. C. Ray, H. M. Tsai, C. W. Pao, F. Z. Chien, W. F. Pong, C. H. Tseng, J. J. Wu, M. H. Tsai, C. H. Chen, H. J. Lin, J. F. Lee and J. H. Guo, *J. Phys. Chem. C*, 2011, **115**, 2650.
- 20 M. Ahmad and J. Zhu, *J. Mater. Chem.*, 2011, **21**, 599.
- 21 Y. Hu, H. H. Qian, Y. Liu, G. H. Du, F. M. Zhang, L. B. Wang and X. Hu, *CrystEngComm*, 2011, **13**, 3438.